TISSUE ENGINEERING: Part C
Volume 21, Number 12, 2015

DOI: 10.1089/ten.tec.2015.0128

termis
Tissue Engineering
& Regenerative Medicine
International Society

METHODS ARTICLE

A Novel Bone Marrow Stimulation Technique Augmented by Administration of Ultrapurified Alginate Gel Enhances Osteochondral Repair in a Rabbit Model

Rikiya Baba, MD,[1] Tomohiro Onodera, MD, PhD,[1] Daisuke Momma, MD,[1] Masatake Matsuoka, MD,[1] Kazutoshi Hontani, MD,[1] Sameh Elmorsy, MD, PhD,[1] Kaori Endo, MD,[1] Masahiro Todoh, PhD,[2] Shigeru Tadano, PhD,[2] and Norimasa Iwasaki, MD, PhD[1]

Cartilage injuries are a common health problem resulting in the loss of daily activities. Bone marrow stimulation technique, one of the surgical techniques for the cartilage injuries, is characterized by technical simplicity and less invasiveness. However, it has been shown to result in fibrous or fibrocartilaginous repair with inferior long-term results. This study focused on using ultrapurified alginate gel (UPAL gel) as an adjuvant scaffold in combination with a bone marrow stimulation technique. The objective of this study was to assess the efficacy of a bone marrow stimulation technique augmented by UPAL gel in a rabbit osteochondral defect model. To achieve this goal, three experimental groups were prepared as follows: defects without intervention, defects treated with a bone marrow stimulation technique, and defects treated with a bone marrow stimulation technique augmented by UPAL gel. The macroscopic and histological findings of the defects augmented by UPAL gel improved significantly more than those of the others at 16 weeks postoperatively. The combination technique elicited hyaline-like cartilage repair, unlike bone marrow stimulation technique alone. This combination procedure has the potential of improving clinical outcomes after use of a bone marrow stimulation technique for articular cartilage injuries.

Introduction

Cartilage injuries are a common health problem, affecting patients in all age groups. According to recent studies, these lesions were found in 61–67% of the patients with symptomatic knees who underwent arthroscopy.[1–3] A localized, full-thickness cartilage lesion classified as ICRS grade 3 or 4 was observed in 17% of all patients diagnosed as having a cartilage lesion.[3] Because of the aging society and the increase in sports participation, the prevalence rate is presumed to be rising. As early as 1743, Hunter observed that cartilage once destroyed, (cartilage) is not repaired.[4] Although various kinds of treatments have been designed to promote cartilage repair,[5–8] their clinical efficacy remains controversial. In the midst of growing expansion of public needs, establishing a novel procedure for cartilage repair close to normal tissue is an urgent issue to improve life and sports activities in patients.

Bone marrow stimulation techniques, such as drilling or microfracture, are characterized by technical simplicity and less invasiveness.[9–11] Therefore, not only young athletes but also middle-aged and older patients have been treated with these techniques.[12] However, bone marrow stimulation techniques have been considered to result in fibrous or fibrocartilaginous repair due to poor recruitment and differentiation of bone marrow-derived mesenchymal stem cells (BM-MSCs), leading to unsatisfactory long-term clinical results.[13–17] To improve postoperative outcomes, technical improvements are required to achieve tissue repair with hyaline or hyaline-like cartilage.

The authors developed an injectable ultrapurified alginate gel (UPAL gel) as a scaffold material for cartilage tissue engineering.[18,19] In the purification process, the contained endotoxin level of UPAL gel was reduced to 5.76 EU/g, whereas that of commercial grade alginate (Sodium Alginate 500, 199–09961; Wako, Osaka, Japan) is 75,950 EU/g.[18] This material can instantaneously gelate as an *in situ* forming gel and enhance the cellular proliferation and chondrogenic differentiation of BM-MSCs, resulting in better reparative tissues in rabbit osteochondral defects.[18,20–22] In addition, UPAL gel containing a chemokine enhanced the recruitment of BM-MSCs and successfully achieved

[1]Department of Orthopaedic Surgery, Hokkaido University Graduate School of Medicine, Sapporo, Japan.
[2]Division of Human Mechanical Systems and Design, Faculty of Engineering, Hokkaido University, Sapporo, Japan.

hyaline-like cartilage repair without exogenous BM-MSC transplantation.[19]

Based on these previous results, we hypothesized that bone marrow stimulation techniques augmented by UPAL gel could induce hyaline-like cartilage regeneration. The objective of this study was to assess the efficacy of this surgical strategy using a rabbit osteochondral defect model. The obtained data will give support to the clinical reality of one-step, minimally invasive, cartilage tissue regenerative medicine without harvesting donor cells.

Materials and Methods

Preparation of alginate gel

An *in situ* forming material based on UPAL gel with a molecular weight of 1700 kDa (Sea Matrix®; Mochida Pharmaceutical Co. Ltd., Tokyo, Japan), which we developed,[18] was used in this experiment. The current material was filter sterilized through a 0.22-mm pore size filter and then freeze-dried for packaging in a sterilized vial. In this study, 2% w/v sodium alginate solution dissolved with normal saline was used.

Rabbit cartilage repair model

Thirty male Japanese white rabbits (3.3–3.7 kg) aged 9 months were anesthetized by an intravenous injection of 0.05 mg/kg of pentobarbital, followed by isoflurane in oxygen gas anesthesia. Their bilateral legs were then shaved and draped in a sterile manner. After a 2-cm anteromedial skin incision was made, the patella was everted through a small, medial parapatellar approach. Using a power drill (Rexon, Kawasaki, Japan), a full-thickness osteochondral defect, 4.0 mm in diameter and 2.0 mm in depth, was created in the patellar groove of each knee. In this study, an originally developed drill sleeve was used to make their depth uniform. For the bone marrow stimulation technique, seven holes were drilled into the defect using a 0.5-mm-diameter drill. The osteochondral defects were divided into three groups as follows ($n = 20$ defects in 20 knees in each group): defects without intervention (group D, Fig. 1A); defects with the bone marrow stimulation technique mentioned above (group MS, Fig. 1B); and defects with the bone marrow stimulation technique augmented by UPAL gel (group MSG, Fig. 1C). In group MSG, the defects were filled with 2% sodium alginate solution after the bone marrow stimulation technique. The alginate solution did not flow out from the defect because of its high viscosity. To avoid excessive exposure to cytotoxic $CaCl_2$, it was injected onto the surface of the alginate for 10 s, and then the superficial layer of alginate was immediately gelated (Fig. 1C). The knees were irrigated with normal saline to wash away the $CaCl_2$ solution. To confirm the stability of the implanted UPAL gel, the knees operated on were intraoperatively flexed and extended 10 times in condition of getting the patella back to its original position. Without any additional fixation to the augmentation site, the capsule and skin were closed with 4–0 black nylon sutures. The rabbits were allowed to move freely in their cages. At 4 and 16 weeks after the operation, 30 defects in 30 knees were evaluated at each time point. Ten defects in each group were used for macroscopic evaluation at each period of time. Five of them were histologically evaluated, and the remaining five were assessed for mechanical properties and subchondral bone repair (Fig. 2).

Macroscopic, histological, and immunohistochemical evaluations

At 4 and 16 weeks after the operation, the animals were euthanized for further investigations. The knee samples were obtained and photographed with a digital camera for macroscopic evaluation. The specimens were prepared for histological and immunohistochemical analyses. A 5-μm-thick section was obtained from the center portion of each defect. The sections were stained with safranin-O and hematoxylin and eosin (HE). To quantitatively evaluate the reparative tissue in each group, macroscopic and histological findings were scored with the 8-point and 28-point grading scales of

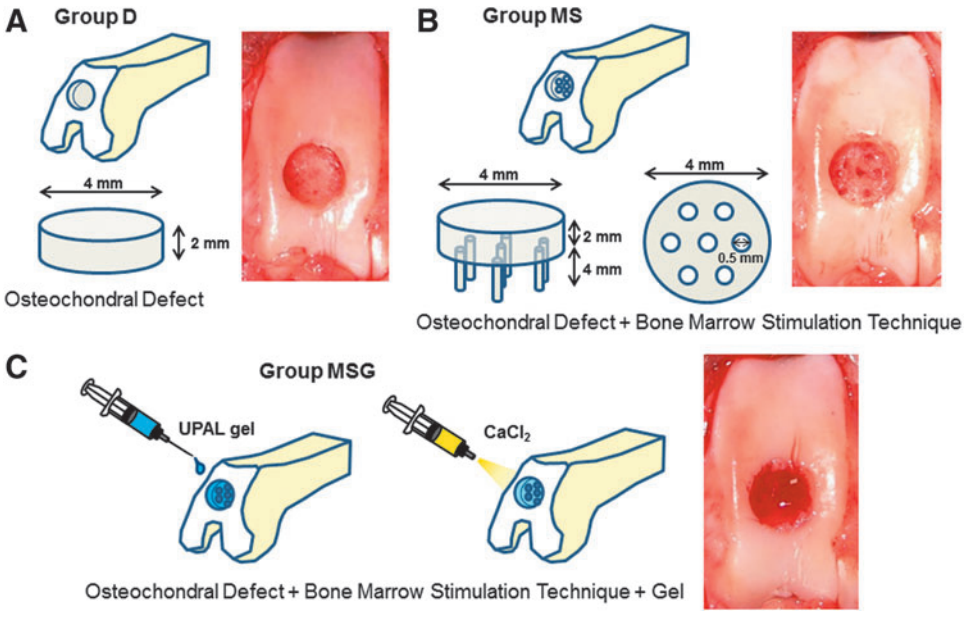

FIG. 1. The procedures for the bone marrow stimulation technique and the injectable implantation system using ultrapurified alginate gel (UPAL gel). A cylindrical defect is created on the patellar groove **(A)**, seven holes of subchondral penetration are made in the defect **(B)**, followed by gelation of the superficial layer of the implanted alginate by applying $CaCl_2$ **(C)**. Color images available online at www.liebertpub.com/tec

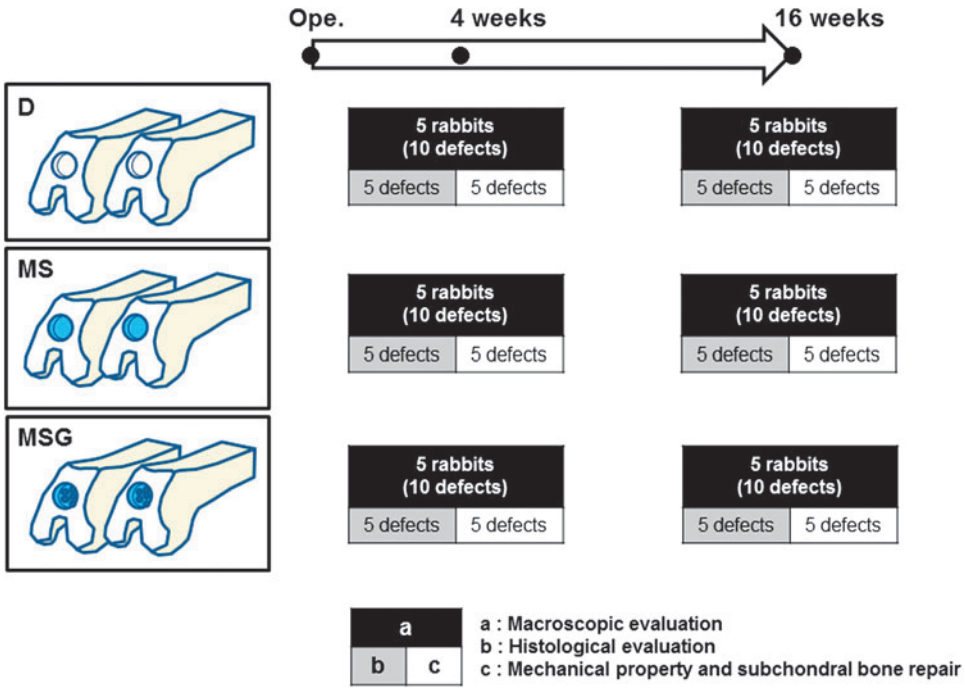

FIG. 2. Experimental design for rabbit cartilage repair models. An osteochondral defect was created bilaterally on the patellar groove. The samples were divided into three groups ($n = 20$ defects in each group). At 4 and 16 weeks after the operation, 10 defects in each group at each period of time were used for macroscopic evaluation. Five of these were histologically evaluated, and the remaining five were assessed for subchondral bone repair and mechanical property. Color images available online at www.liebertpub.com/tec

Niederauer *et al.* (Tables 1 and 2),[23] which are a modification of the scoring system reported by O'Driscoll.[24] The scores were determined by an independent blinded observer. To avoid observer bias, the samples were randomized and coded before analysis. Immunohistochemical staining was performed with anti-type I and anti-type II collagen antibodies (Fuji Pharm. Lab., Toyama, Japan). For quantitative evaluation of glycosaminoglycan (GAG) content, the findings of safranin-O staining were scored using the three-point grading scales of Mohan's scoring system.[25]

Evaluation of the collagen orientation by a polarized light microscope

To evaluate the collagen orientation of the repaired tissue at 16 weeks postoperatively, a supplemental evaluation using a polarized light microscope (PLM) (ECLIPSE E600 POL; Nikon, Tokyo, Japan) was conducted.[26–28] This evaluation was carried out on HE-stained sections in each group. Two cross polarizers were used so that highly ordered collagen perpendicular to the articular surface appeared bright, while collagen that is not ordered (nonbirefringent) appears darkest. The contrast of fibrils oriented more parallel to the articular surface was darker than for collagen perpendicular to the articular surface. To observe the predominant direction of birefringent regions and confirm the lack of orientation in nonbirefringent regions, the sections were rotated 0°, 45°, and 90° with respect to the fixed filters. Microscopic images were acquired through a digital camera (DS-5M-L1; Nikon). Each sample was independently examined by an experienced PLM user. To quantitatively evaluate the results, the findings were assessed by the PLM qualitative score, which was reported by Changoor *et al.* (Table 3).[29] The scores were determined by an independent blinded observer. To avoid observer bias, the slides were randomized and coded before analysis.

Table 1. Macroscopic Score[23]

Edge integration into native cartilage	
Full	2
Partial	1
None	0
Smoothness of the cartilage surface	
Smooth	2
Intermediate	1
Rough	0
Cartilage surface, degree of filling	
Flush	2
Slight depression	1
Depressed/Overgrown	0
Color of cartilage, opacity, or translucency of the Neocartilage	
Transparent	2
Translucent	1
Opaque	0

Microcomputed tomography evaluation of subchondral bone repair

To compare the degree of subchondral bone repair in each group, the harvested tissues were evaluated with a microcomputed tomography (micro-CT) scanner (R_mCT2; Rigaku, Tokyo, Japan) at 20 μm/pixel. The imaging conditions of micro-CT were 80 kV and 100 μA. The images were processed with ImageJ software (National Institutes of Health, Bethesda, MD), and quantitative three-dimensional bone analyses were performed using the Bone J plugin for ImageJ.[30] Regions of interest were manually set at the original cylindrical defect area (4.0 mm in diameter and 2.0 mm in depth). The threshold levels of gray values were uniformly set for all samples. The lower threshold value chosen for the binary image was determined to be that which mimicked bone as closely as possible compared with the raw image. The volume of mineralized bone, which is

Table 2. Histological Score[23]

Nature of predominant tissue	
Hyaline cartilage	4
Mostly hyaline cartilage	3
Mixed hyaline and fibrocartilage	2
Mostly fibrocartilage	1
Some fibrocartilage, mostly nonchondrocytic cells	0
Structural characteristics	
Surface regularity	
Smooth and intact	3
Superficial horizontal lamination	2
Fissures	1
Severe disruption, including fibrillation	0
Structural integrity, homogeneity	
Normal	2
Slight disruption	1
Severe disintegration, disruptions	0
Thickness	
100% of adjacent cartilage	2
50–100% of normal cartilage	1
0–50% of normal cartilage	0
Bonding to adjacent cartilage	
Bonded at both ends of graft	2
Bonded at one end or partially at both ends	1
Not bonded	1
Freedom from cellular changes of degeneration	
Hypocellularity	
Normal cellularity	2
Slight hypocellularity	1
Moderate hypocellularity or hypercellularity	0
Chondrocyte clustering	
No clusters	2
<25% of the cells	1
25–100% of the cells	0
Freedom from degenerative changes in adjacent cartilage	
Normal cellularity, no clusters, normal staining	3
Normal cellularity, mild clusters, moderate staining	2
Mild or moderate hypo/hypercellularity, slight staining	1
Sever hypocellularity, poor or no staining	0
Subchondral bone	
Reconstruction of subchondral bone	
Normal	3
Reduced subchondral bone reconstruction	2
Minimal subchondral bone reconstruction	1
No subchondral bone reconstruction	0
Inflammatory response in subchondral bone region	
None/mild	2
Moderate	1
Severe	0
Safranin-O staining	
Normal or near normal	3
Moderate	2
Slight	1
None	0

defined as the repaired bone volume (BV), and bone mineral density (BMD) in the region of interest were calculated.

Evaluation of mechanical properties

The mechanical properties of each sample prepared for assessment of subchondral bone repair were measured using indentation test equipment designed by our laboratory for small samples, which was attached to a material testing machine (AGS-H; Shimazu, Kyoto, Japan). The specimens were mounted solidly and placed with the articular surface facing up into a rod with a flat nonporous indenter (2.0 mm in diameter). The tests were done at room temperature. An indenter moved (0.5 mm/min) automatically toward the center of the reparative tissue. The load (N) and displacement (mm) curves were recorded, and then the stiffness (N/mm) was obtained from the linear region of the curve.

Data analyses

All data are presented as mean ± standard deviation. To determine the sample size, based on previous studies using UPAL gel,[18,19] we performed power analyses in advance (data are not shown). Significant differences among the three groups were evaluated by nonparametric Kruskal–Wallis tests between groups. Comparisons between two groups were performed by paired *t*-tests. Statistical analyses were performed using JMP Pro version 10.0 statistical software (SAS Institute, Cary, NC). Significance was accepted with a p-value <0.05.

Results

Macroscopic morphology

There were no perioperative complications and no macroscopic signs indicating infection, including excessive joint fluid or purulent synovitis in any knees, at each time point. At 4 weeks postoperatively, the surfaces of the reparative tissues in group D were rough and depressed. Those in group MS and group MSG were somewhat rough and moderately depressed (Fig. 3A–C). The macroscopic scores were significantly higher for group MS (mean ± SD; 1.70 ± 0.95, $p = 0.0134$) and group MSG (2.30 ± 1.82, $p = 0.0058$) than for group D (0.40 ± 0.70) (Fig. 3G).

At 16 weeks postoperatively, the surfaces of the reparative tissues in group D and group MS remained somewhat rough, slightly depressed, and poorly integrated with the adjacent cartilage (Fig. 3D, E). On the other hand, those in group MSG were smooth and showed good integration with the adjacent cartilage (Fig. 3F). The macroscopic scores of group MSG (5.60 ± 1.17) were significantly higher than those of group D (2.20 ± 1.03, $p = 0.0005$) and group MS (3.50 ± 1.18, $p = 0.0057$) (Fig. 3H). Mean total macroscopic scores improved significantly from 4 to 16 weeks postoperatively in all groups ($p = 0.0002$ in the group D, $p = 0.0008$ in the group MS, $p = 0.0001$ in the group MSG). No other significant differences in the scores were found among the groups.

Histological and immunohistochemical findings

At 4 weeks after the operation, the defects in group D were filled with fibrous tissues, including fibroblastic cells (Fig. 4A, D, G). In group MS, although a few chondrocytic cells were observed in the peripheral zone of the defects, the defects were mostly filled with fibrous tissues mainly containing type I collagen (Fig. 4B, E, H). On the other hand, the defects in group MSG were partially filled with hyaline-like cartilaginous tissue containing GAG matrix and type II collagen (Fig. 4C, F, I). The histological scores tended to be higher for group MSG (7.20 ± 1.92) than for group D (5.40 ± 2.88) and group MS (5.60 ± 1.52), but the differences were not significant (Fig. 4J).

Table 3. The Polarized Light Microscopy Qualitative Score[29]

Score	*Description*
0	Evidence of fiber organization, seen as sparse bright patches throughout the specimen. These patches do not have parallel alignment at the surface of the specimen nor perpendicular alignment in the deep zone (DZ), but are randomly oriented in the specimen.
1	Birefringent tissue of the expected orientation in the DZ with fibers oriented mainly perpendicular (±30) to the cartilage–bone interface and occupying less than ~50% of the thickness of the noncalcified tissue on average. Little additional evidence of birefringent tissue is apparent, other than randomly oriented patches. Birefringent tissue may have inconsistent thickness and intensity of birefringence across the lateral direction of the specimen. The specimen texture may be smooth, patchy, or granular.
2	Identical to a score of 1 except that the DZ occupies more than ~50% of the thickness of the noncalcified tissue. Alternatively, a second region of birefringent tissue may be present above the DZ that may have any orientation (parallel to the articular surface, obliquely oriented to the articular surface, or multiple orientations) except for vertical. In this case, the DZ may then occupy <50% of the thickness of the noncalcified tissue.
3	Zonal organization with birefringent tissue in the DZ perpendicular to the cartilage–bone interface (±30), and birefringent tissue at the articular surface that is either aligned parallel to the surface or that has multiple orientations. These two zones are separated by a third nonbirefringent region that is appropriate to the species from which the specimen was taken; for example, in human articular cartilage, it may be a thin nonuniform region that is difficult to distinguish compared with the consistent dark band observed in equine articular cartilage. Alternatively, the two birefringent zones are separated by a birefringent region with orientation that is neither parallel nor perpendicular. Zonal thicknesses are heterogeneous across the lateral direction of the specimen. The specimen texture may be smooth, patchy, or granular.
4	Identical to a score of 3 except that the orientation in the superficial zone (SZ) must be parallel to the surface and the transitional zone (TZ) must be appropriate to the species from which the specimen was taken; for example, in human articular cartilage, it may be a thin nonuniform region that is difficult to distinguish compared with the consistent dark band observed in equine articular cartilage. In addition to these characteristics, each zone should approximate the zonal proportions for the species from which the specimen was taken; for example, in human articular cartilage, the DZ should be the largest, occupying >50% of the total thickness of noncalcified tissue. The transitional and SZs are smaller and the TZ may be larger than the SZ.
5	Displays birefringence patterns of young adult hyaline articular cartilage with distinct, superficial, and deep zones with uniform birefringence, indicating parallel and perpendicularly oriented fibers, respectively, separated by an appropriate TZ. Zonal thicknesses are appropriate for the species and location from which the specimen was taken and are relatively homogeneous across the lateral direction of the specimen. Overall, the specimen birefringence has a uniform smooth texture and is neither granular nor patchy.

At 16 weeks postoperatively, the defects in group D were filled with fibrous tissues with a severely disrupted surface (Fig. 5A, D, G). In group MS, the defects were mostly filled with fibrocartilage and some disruptions were detected (Fig. 5B, E, H). Moreover, the reparative tissues in groups D and MS contained mainly type I collagen-positive staining matrix (Fig. 5D, E). In contrast, reparative tissues in group MSG were mostly hyaline-like cartilage with rich GAG matrix content and strong type II collagen staining (Fig. 5C, I). The histological scores were significantly higher for group

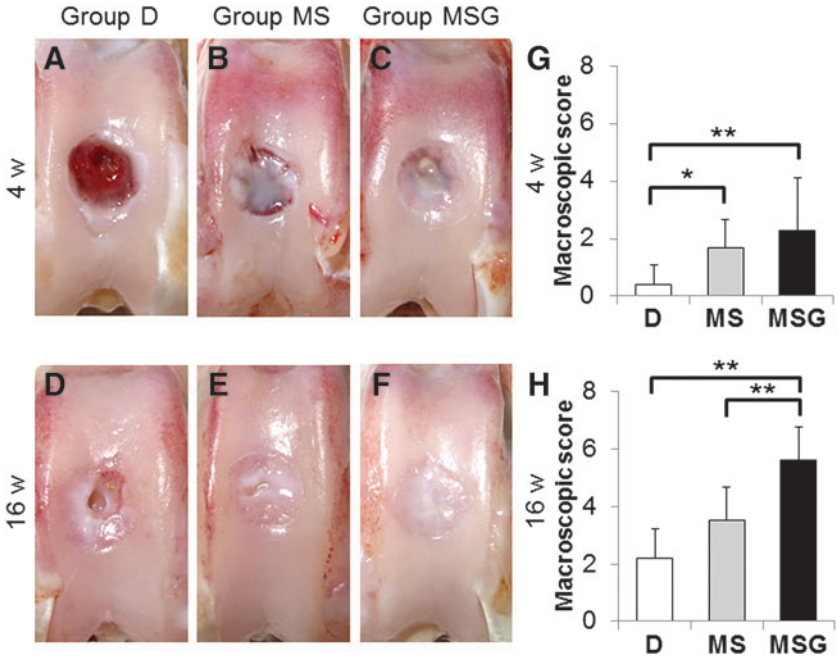

FIG. 3. Macroscopic morphology of the osteochondral defect at 4 weeks **(A–C)** and 16 weeks **(D–F)** postoperatively. Macroscopic scores at 4 weeks **(G)** and 16 weeks **(H)** postoperatively ($n = 10$ at each time point). Values are mean and SD. $*p < 0.05$, $**p < 0.01$. Color images available online at www.liebertpub.com/tec

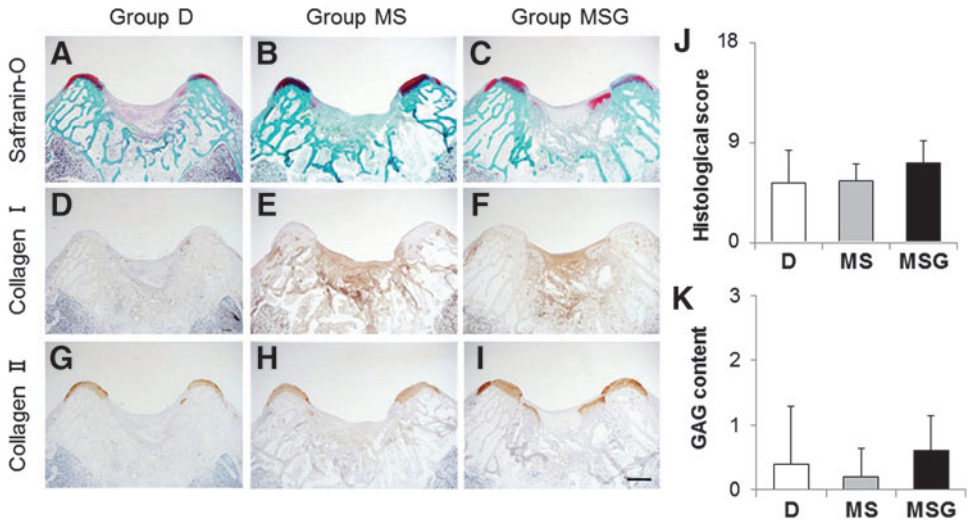

FIG. 4. Histological sections of osteochondral defects at 4 weeks after the operation. Sections were stained with safranin-O **(A–C)** and immunohistochemically stained with anti-type I **(D–F)** and anti-type II **(G–I)** collagen antibodies. Scale bar: 1 mm. **(J)** Histological scores at 4 weeks postoperatively ($n=5$). Niederauer's histological scoring scale range: 0–28. Histological scores for glycosaminoglycan (GAG) content **(K)** at 4 weeks postoperatively ($n=5$). Scoring scale range: 0–3. Values are mean and SD. Color images available online at www.liebertpub.com/tec

MSG (13.60 ± 2.88) than for group D (5.20 ± 2.05, $p=0.0234$) and group MS (7.00 ± 3.08, $p=0.0422$) (Fig. 5J).

Collagen orientation of the reparative tissue

At 16 weeks after the operation, the sections in groups D and MS viewed with a PLM showed no organization of vertically oriented deep zones (Fig. 6B–D, F–H). On the other hand, vertically oriented deep zones and additional two zones approximating the transitional and superficial zones were found in the sections of group MSG (Fig. 6J–L). In addition, the vertically oriented collagen fibers in the deep zone were well integrated with the underlying subchondral bone. However, the transitional zone was smaller than the superficial zone, and the zonal thickness was not completely homogeneous (Fig. 6K), which is contrary to the normal cartilage (Fig. 6N–P). Although the collagen orientations of the reparative tissue in group MSG were not completely organized like a normal cartilage, the PLM scores in group MSG (2.00 ± 1.00) were significantly better than those in group D (0.20 ± 0.45, $p=0.0315$) and group MS (0.20 ± 0.45, $p=0.0315$) (Fig. 6Q).

Subchondral bone repair

At 4 weeks after the operation, there was little reconstruction of subchondral bone in all of the interventional defects. The volumes of repaired subchondral bone evaluated by micro-CT were significantly less in all experimental groups ($1.32 \pm 0.69\,mm^3$ in group D, $p=0.0447$; $1.31 \pm 1.49\,mm^3$ in group MS, $p=0.0447$; $1.36 \pm 0.66\,mm^3$ in group MSG, $p=0.0447$) than in normal distal femur ($13.52 \pm 0.82\,mm^3$) (Fig. 7E). In addition, BMDs in all experimental groups ($483.43 \pm 6.24\,mg/cm^3$ in group D, $p=0.0447$; $475.57 \pm 5.31\,mg/cm^3$ in group MS, $p=0.0447$; $489.73 \pm 11.37\,mg/cm^3$ in group MSG, $p=0.0447$) were significantly lower than those in normal distal femur ($567.04 \pm 7.12\,mg/cm^3$) (Fig. 7G). At 16 weeks after the operation, although the subchondral bone in the defects of group D (Fig. 7A) was repaired partially, those of groups MS (Fig. 7B) and MSG (Fig. 7C) were mostly repaired, except for the central part of the defect. In addition, excessive bone ingrowth into the defect was not observed in any groups. The repaired subchondral BVs of group MS ($9.53 \pm 1.92\,mm^3$) and group MSG ($9.74 \pm 3.97\,mm^3$) tended to be higher than those of group D ($8.33 \pm 1.52\,mm^3$). However, no significant differences

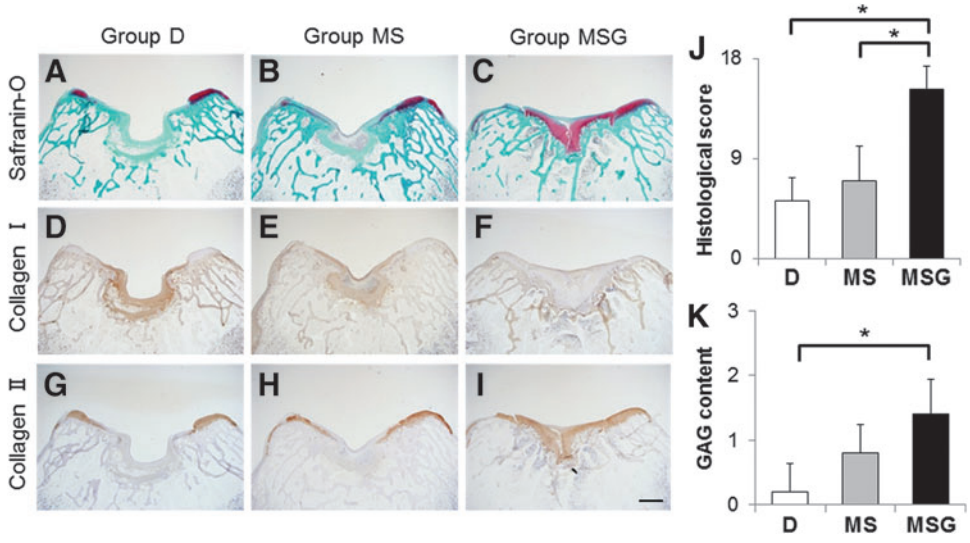

FIG. 5. Histological sections of osteochondral defects at 16 weeks after the operation. Sections were stained with safranin-O **(A–C)** and immunohistochemically stained with anti-type I **(D–F)** and anti-type II **(G–I)** collagen antibodies. Scale bar: 1 mm. **(J)** Histological scores at 16 weeks postoperatively ($n=5$). Niederauer's histological scoring scale range: 0–28. Histological scores for GAG content **(K)** at 16 weeks postoperatively ($n=5$). Scoring scale range: 0–3. Values are mean and SD. *$p<0.05$. Color images available online at www.liebertpub.com/tec

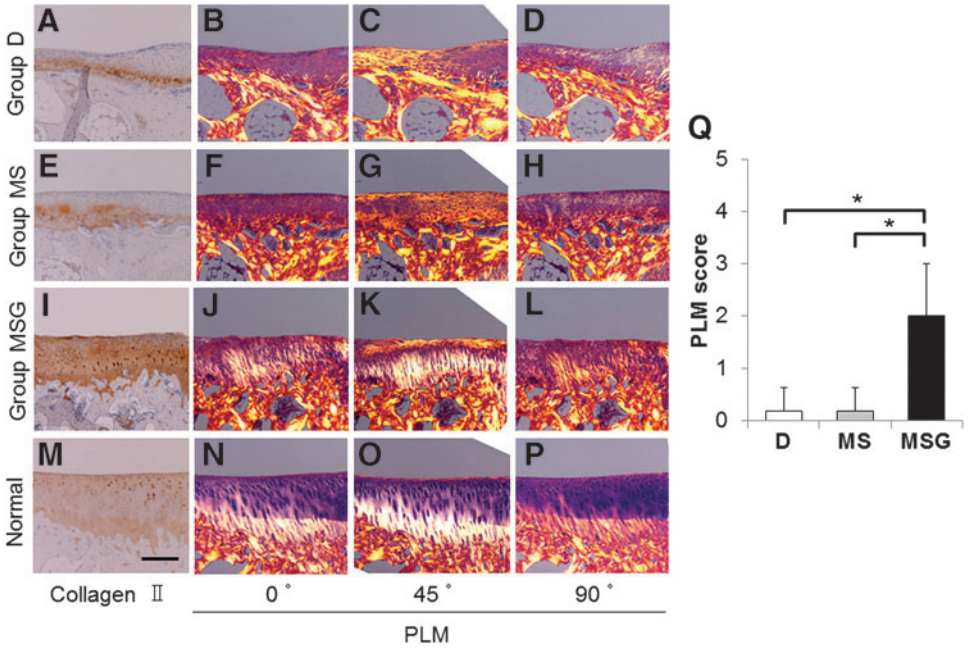

FIG. 6. The evaluation for the collagen orientation of reparative tissues at 16 weeks after the operation. Sections **(A, E, I, M)** were immunohistochemically stained with anti-type II collagen antibodies. Scale bar: 250 μm. The sections stained with HE **(B–D, F–H, J–L, N–P)** were viewed with a polarized light microscope (PLM) at multiple angles (0°, 45°, 90°). **(Q)** The PLM qualitative scores (scoring scale range: 0–5) at 16 weeks postoperatively ($n=5$). Values are mean and SD. $^*p<0.05$. Color images available online at www.liebertpub.com/tec

in the volumes were found among the experimental groups (Fig. 7F). BMDs in all experimental groups ($551.74\pm28.09\,mg/cm^3$ in group D; $555.46\pm29.16\,mg/cm^3$ in group MS; $571.28\pm24.16\,mg/cm^3$ in group MSG) almost reached that in normal distal femur ($567.04\pm7.12\,mg/cm^3$); furthermore, there were no significant differences between experimental groups and normal distal femur (Fig. 7H).

Measurements of mechanical properties

The indentation testing was conducted for the samples at 16 weeks postoperatively and for normal patellar grooves as controls ($n=5$). Since the defects of group D were not covered with sufficient reparative tissues, they were excluded from the measurements. The representative mechanical plots for

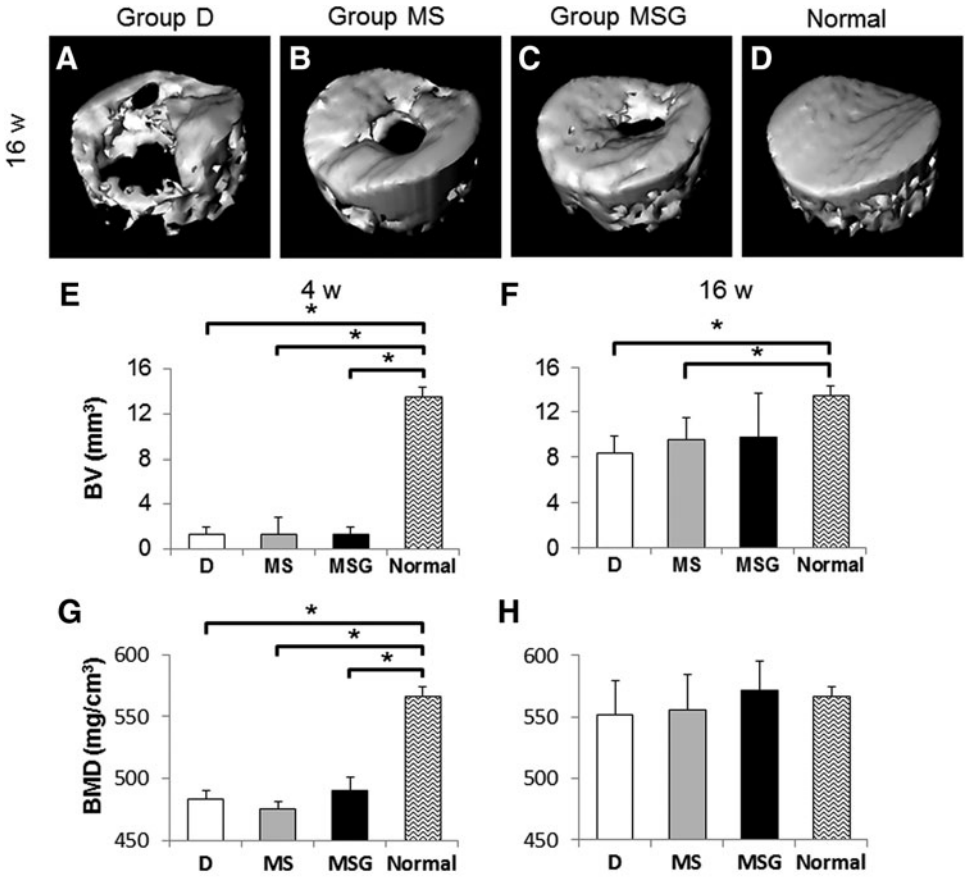

FIG. 7. Evaluations for subchondral bone repair by microcomputed tomography (micro-CT). Representative three-dimensional CT images at 16 weeks postoperatively **(A–D)** from each group ($n=5$) are shown. Repaired subchondral bone volume (BV) **(E, F)** and bone mineral density (BMD) **(G, H)** were assessed at 4 weeks **(E, G)** and 16 weeks **(F, H)** postoperatively. Values are mean and SD. $^*p<0.05$.

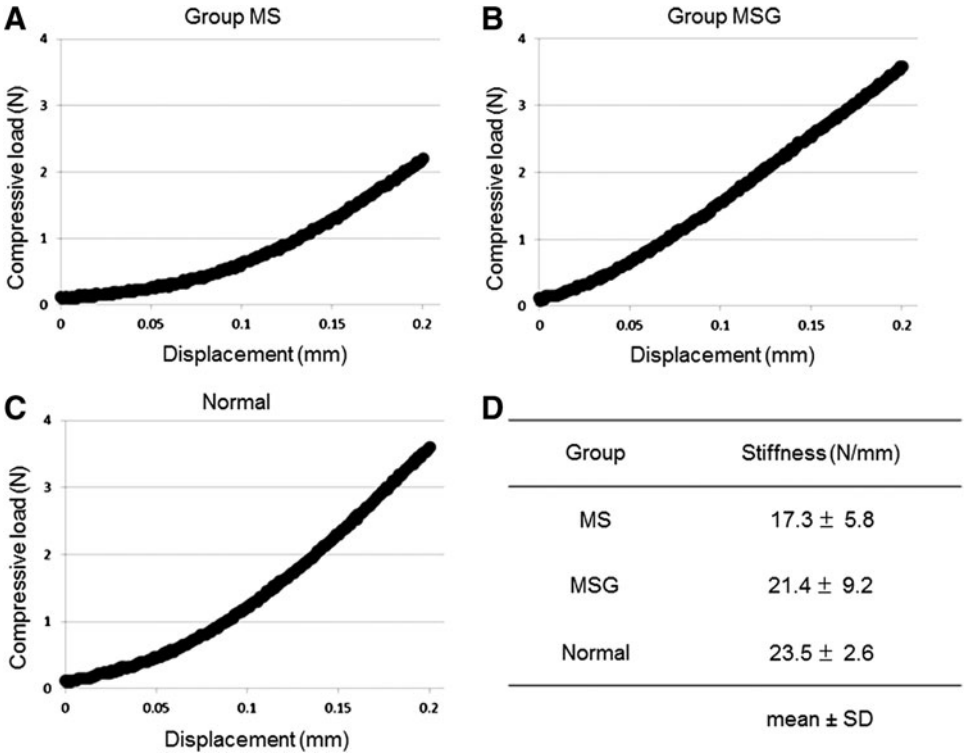

FIG. 8. The results of indentation testing at 16 weeks postoperatively. Representative mechanical plots from each group **(A–C)** are shown. The stiffness (N/mm) **(D)** was obtained from the linear region of the load/displacement curve.

samples in each group are shown in Figure 8A–C. The stiffness (N/mm) was obtained from the linear region (0.125–0.200 mm) of the curve ($R^2 = 0.997 \pm 0.001$ in group MS, $R^2 = 0.993 \pm 0.007$ in group MSG, $R^2 = 0.998 \pm 0.002$ in normal cartilages). The mean stiffness of group MSG (21.4 ± 9.2 N/mm) and group MS (17.3 ± 5.8 N/mm) reached $\sim$91% and 74% of that of normal cartilages (23.5 ± 2.6 N/mm), respectively (Fig. 8D). No significant differences were found among the three groups.

Discussion

The objective of this study was to assess the efficacy of a bone marrow stimulation technique augmented by UPAL gel. Compared with a bone marrow stimulation technique alone, the combination of this technique and administration of UPAL gel significantly improved the macroscopic and histological findings, including the collagen orientation of reparative tissues in a rabbit osteochondral defect model. Moreover, the mechanical properties of reparative tissues in the combined group tended to be close to those of normal cartilage. Based on these results, we concluded that UPAL gel accelerated cartilage repair containing abundant GAG and the organized type II collagen when combined with a bone marrow stimulation technique.

For cartilage tissue engineering, several procedures augmented by biomaterials have recently been introduced to enable a one-step operation without cell implantation.[31–35] These procedures successfully accelerated cartilage repair, except for one report of excessive osteogenesis.[36] Therefore, the previous studies suggest that the combination of bone marrow stimulation and scaffold augmentation is a promising strategy to enhance hyaline-like cartilage repair, unless it induces excessive osteogenesis. To stabilize the scaffold *in situ*, several procedures require fixation materials. Anders *et al.* fixated a bilayer matrix of porcine type I/III collagen with sutures or glue.[31] Siclari *et al.* stabilized textile polyglycolic acid–hyaluronan implants with biodegradable pins or glue.[33] Although these procedures showed enhancement of cartilage repair, the fixation materials have a potential for negative effects on cartilage repair or biotic organisms, and it is preferable not to use materials at the injury site.[37–39]

Recent reports showed new techniques to stabilize the scaffold without fixation materials. Efe *et al.* implanted a round type I collagen gel matrix derived from rat tails in a press-fit manner.[34] In this technique, it is necessary to make the fixed size defect before the implantation of the scaffold. Stanish *et al.* stabilized chitosan-glycerol phosphate/blood implants by *in situ* coagulation, utilizing the characteristic that it is solidified within a few minutes after mixing with whole blood.[35] Although these techniques that did not use fixation materials are less invasive, ideally, a simpler and quicker technique is desirable. UPAL gel can immediately form a gel by contact with Ca^{2+}. Instant stabilization and structural compatibility of UPAL gel are great advantages in the clinical situation, especially in an arthroscopic technique.

In the current study, the UPAL gel augmentation elicited hyaline-like cartilage repair. We previously confirmed that host cells from bone marrow were able to penetrate into the defect filled with UPAL gel, and local administration of SDF-1 enhanced host cell migration.[19] Regarding the structural characteristics of UPAL gel, the surface is gelated, whereas the inside remains in a solution state in an osteochondral defect. Bone marrow stimulation may have enhanced host cell recruitment into the defects filled with alginate solution. Subsequently, host cells accumulated in the defects because of the coverage of the gelated surface. In addition, this hydrogel is capable of enhancing cellular

proliferation and chondrogenic differentiation.[18] Therefore, the recruited host cells successfully proliferated and differentiated into chondrocytes after penetration.

There was a concern that UPAL gel would inhibit subchondral bone repair instead of accelerating chondrogenic differentiation. Furthermore, the acceleration of cell recruitment into the defects may cause adverse effects such as cartilage formation or scarring into the subchondral bone.[40] Therefore, subchondral bone repair was evaluated quantitatively by micro-CT. Subchondral bone loss due to excess scar formation or ectopic chondrogenesis was not observed in the UPAL gel augmentation group. No apparent difference in the repaired subchondral BVs was found between the UPAL gel augmentation group and the bone marrow stimulation group. BMDs were almost equal in all experimental groups at 4 and 16 weeks. This finding implies that UPAL gel augmentation does not affect calcification during the process of subchondral bone healing. Moreover, the indentation test revealed that the stiffness of reparative tissues in the UPAL gel augmentation group was much closer to that in normal osteochondral tissue compared with that in the bone marrow stimulation group. These results indicate that UPAL gel augmentation enhances cartilage regeneration without disturbance of subchondral bone repair.

In the current study, the histological score of the defect augmented by UPAL gel showed 49% of the full score and that of the defect without intervention was 19% of the full score at 16 weeks postoperatively. In contrast, in a previous study using immature rabbits, the histological score of the defect filled with UPAL gel containing BM-MSCs reached 59% of the full score and that of the defect without intervention was 24% of the full score at 12 weeks postoperatively.[18] Although osteochondral defects of younger rabbits are known to repair more easily than those of mature rabbits,[41–43] skeletally mature rabbits were used here to emulate the clinical situation in humans.[44–46] Therefore, UPAL gel was applied to mature rabbits in this study, and the reparative tissues of mature rabbits were less than those of previous studies. Moreover, the defects were created in a partly weight-bearing region.[42] Hence, there is a possibility of the lack of the appropriate mechanical stimulus resulting in insufficient subchondral bone repair.[47] Because the synthesis of hyaline-like cartilage is accompanied with a viable subchondral bone,[45] insufficient subchondral bone repair in this study is one of the reasons for the unsatisfactory cartilage repair. Although our results indicated that the UPAL gel augmentation did not prevent the subchondral bone repair, an additional treatment for subchondral bone repair should be performed when there is a deep osteochondral defect. In addition, since osteogenesis in the weight-bearing region might be larger than in the less weight-bearing region, further research using UPAL gel will be needed if there is a defect located in the weight-bearing region. The present results imply that close consideration of patient age and injury size is needed when UPAL gel is applied in the future.

There were several limitations in this study. First, the results were obtained from a rabbit model. Considering the clinical application of UPAL gel, histological and biomechanical analyses based on a large animal model should be performed. Second, the *in vivo* metabolic pathway of UPAL gel was not clarified here. Although Igarashi *et al.* demonstrated that the UPAL gel was completely diminished between 2 and 4 weeks after implantation in living joints,[18] the elucidation of the metabolic pathway is essential to use this hydrogel clinically.

In conclusion, a bone marrow stimulation technique augmented by UPAL gel demonstrated favorable effects on the reparative process in rabbit osteochondral defects. This strategy as an acellular treatment option has the potential to improve the clinical outcome after bone marrow stimulation without loss of its technical simplicity and cost effectiveness.

Acknowledgments

This work is supported, in part, by the Newly Extended Technology Transfer Program (NexTEP) of the Japan Science and Technology Agency (JST). The authors are especially thankful to Mr. Shimizu (Mochida Pharmaceutical Co. Ltd.) for material preparations.

Disclosure Statement

No competing financial interests exist.

References

1. Hjelle, K., Solheim, E., Strand, T., Muri, R., and Brittberg, M. Articular cartilage defects in 1,000 knee arthroscopies. Arthroscopy **18,** 730, 2002.
2. Widuchowski, W., Widuchowski, J., and Trzaska, T. Articular cartilage defects: study of 25,124 knee arthroscopies. Knee **14,** 177, 2007.
3. Aroen, A., Loken, S., Heir, S., Alvik, E., Ekeland, A., Granlund, O.G., and Engebretsen, L. Articular cartilage lesions in 993 consecutive knee arthroscopies. American J Sports Med **32,** 211, 2004.
4. Hunter, W. Of the structure and diseases of articulating cartilages, by William Hunter, surgeon. Philos Trans **42,** 514, 1742.
5. Pridie, K.H. A method of resurfacing osteoarthritis knee joints. J Bone Joint Surg Br **41,** 618, 1959.
6. Matsusue, Y., Yamamuro, T., and Hama, H. Arthroscopic multiple osteochondral transplantation to the chondral defect in the knee associated with anterior cruciate ligament disruption. Arthroscopy **9,** 318, 1993.
7. Brittberg, M., Lindahl, A., Nilsson, A., Ohlsson, C., Isaksson, O., and Peterson, L. Treatment of deep cartilage defects in the knee with autologous chondrocyte transplantation. N Engl J Med **331,** 889, 1994.
8. Steadman, J.R., Rodkey, W.G., Briggs, K.K., and Rodrigo, J.J. [The microfracture technic in the management of complete cartilage defects in the knee joint]. Orthopade **28,** 26, 1999.
9. Mandelbaum, B.R., Browne, J.E., Fu, F., Micheli, L., Mosely, J.B., Jr., Erggelet, C., Minas, T., and Peterson, L. Articular cartilage lesions of the knee. Am J Sports Med **26,** 853, 1998.
10. Gobbi, A., Nunag, P., and Malinowski, K. Treatment of full thickness chondral lesions of the knee with microfracture in a group of athletes. Knee Surg Sports Traumatol Arthrosc **13,** 213, 2005.
11. Mithoefer, K., Williams, R.J., 3rd, Warren, R.F., Wickiewicz, T.L., and Marx, R.G. High-impact athletics after knee articular cartilage repair: a prospective evaluation of the microfracture technique. Am J Sports Med **34,** 1413, 2006.
12. Goyal, D., Keyhani, S., Lee, E.H., and Hui, J.H. Evidence-based status of microfracture technique: a systematic review of level I and II studies. Arthroscopy **29,** 1579, 2013.

13. Mitchell, N., and Shepard, N. The resurfacing of adult rabbit articular cartilage by multiple perforations through the subchondral bone. J Bone Joint Surg Am **58,** 230, 1976.
14. Shapiro, F., Koide, S., and Glimcher, M.J. Cell origin and differentiation in the repair of full-thickness defects of articular cartilage. J Bone Joint Surg Am **75,** 532, 1993.
15. Buckwalter, J.A. Articular cartilage injuries. Clin Orthop Relat Res 21, 2002.
16. Dorotka, R., Bindreiter, U., Macfelda, K., Windberger, U., and Nehrer, S. Marrow stimulation and chondrocyte transplantation using a collagen matrix for cartilage repair. Osteoarthritis Cartilage **13,** 655, 2005.
17. Hiraki, Y., Shukunami, C., Iyama, K., and Mizuta, H. Differentiation of chondrogenic precursor cells during the regeneration of articular cartilage. Osteoarthritis Cartilage **9 Suppl A,** S102, 2001.
18. Igarashi, T., Iwasaki, N., Kasahara, Y., and Minami, A. A cellular implantation system using an injectable ultrapurified alginate gel for repair of osteochondral defects in a rabbit model. J Biomed Mater Res A **94,** 844, 2010.
19. Sukegawa, A., Iwasaki, N., Kasahara, Y., Onodera, T., Igarashi, T., and Minami, A. Repair of rabbit osteochondral defects by an acellular technique with an ultrapurified alginate gel containing stromal cell-derived factor-1. Tissue Eng Part A **18,** 934, 2012.
20. Mierisch, C.M., Cohen, S.B., Jordan, L.C., Robertson, P.G., Balian, G., and Diduch, D.R. Transforming growth factor-beta in calcium alginate beads for the treatment of articular cartilage defects in the rabbit. Arthroscopy **18,** 892, 2002.
21. Steinert, A., Weber, M., Dimmler, A., Julius, C., Schutze, N., Noth, U., Cramer, H., Eulert, J., Zimmermann, U., and Hendrich, C. Chondrogenic differentiation of mesenchymal progenitor cells encapsulated in ultrahigh-viscosity alginate. J Orthop Res **21,** 1090, 2003.
22. Bian, L., Zhai, D.Y., Tous, E., Rai, R., Mauck, R.L., and Burdick, J.A. Enhanced MSC chondrogenesis following delivery of TGF-beta3 from alginate microspheres within hyaluronic acid hydrogels in vitro and in vivo. Biomaterials **32,** 6425, 2011.
23. Niederauer, G.G., Slivka, M.A., Leatherbury, N.C., Korvick, D.L., Harroff, H.H., Ehler, W.C., Dunn, C.J., and Kieswetter, K. Evaluation of multiphase implants for repair of focal osteochondral defects in goats. Biomaterials **21,** 2561, 2000.
24. O'Driscoll, S.W., Keeley, F.W., and Salter, R.B. The chondrogenic potential of free autogenous periosteal grafts for biological resurfacing of major full-thickness defects in joint surfaces under the influence of continuous passive motion. An experimental investigation in the rabbit. J Bone Joint Surg Am **68,** 1017, 1986.
25. Mohan, N., Dormer, N.H., Caldwell, K.L., Key, V.H., Berkland, C.J., and Detamore, M.S. Continuous gradients of material composition and growth factors for effective regeneration of the osteochondral interface. Tissue Eng Part A **17,** 2845, 2011.
26. Roberts, S., McCall, I.W., Darby, A.J., Menage, J., Evans, H., Harrison, P.E., and Richardson, J.B. Autologous chondrocyte implantation for cartilage repair: monitoring its success by magnetic resonance imaging and histology. Arthritis Res Ther **5,** R60, 2003.
27. Ross, K.A., Williams, R.M., Schnabel, L.V., Mohammed, H.O., Potter, H.G., Bradica, G., Castiglione, E., Pownder, S.L., Satchell, P.W., Saska, R.A., and Fortier, L.A. Comparison of three methods to quantify repair cartilage collagen orientation. Cartilage **4,** 111, 2013.
28. Roberts, S., Menage, J., Sandell, L.J., Evans, E.H., and Richardson, J.B. Immunohistochemical study of collagen types I and II and procollagen IIA in human cartilage repair tissue following autologous chondrocyte implantation. Knee **16,** 398, 2009.
29. Changoor, A., Tran-Khanh, N., Methot, S., Garon, M., Hurtig, M.B., Shive, M.S., and Buschmann, M.D. A polarized light microscopy method for accurate and reliable grading of collagen organization in cartilage repair. Osteoarthritis Cartilage **19,** 126, 2011.
30. Doube, M., Klosowski, M.M., Arganda-Carreras, I., Cordelieres, F.P., Dougherty, R.P., Jackson, J.S., Schmid, B., Hutchinson, J.R., and Shefelbine, S.J. BoneJ: Free and extensible bone image analysis in ImageJ. Bone **47,** 1076, 2010.
31. Anders, S., Volz, M., Frick, H., and Gellissen, J. A randomized, controlled trial comparing autologous matrix-induced chondrogenesis (AMIC(R)) to microfracture: analysis of 1- and 2-year follow-up data of 2 centers. Open Orthop J **7,** 133, 2013.
32. Behrens, P. Matrixgekoppelte Mikrofrakturierung. Arthroskopie **18,** 193, 2005.
33. Siclari, A., Mascaro, G., Gentili, C., Kaps, C., Cancedda, R., and Boux, E. Cartilage repair in the knee with subchondral drilling augmented with a platelet-rich plasma-immersed polymer-based implant. Knee Surg Sports Traumatol Arthrosc **22,** 1225, 2013.
34. Efe, T., Theisen, C., Fuchs-Winkelmann, S., Stein, T., Getgood, A., Rominger, M.B., Paletta, J.R., and Schofer, M.D. Cell-free collagen type I matrix for repair of cartilage defects-clinical and magnetic resonance imaging results. Knee Surg Sports Traumatol Arthrosc **20,** 1915, 2012.
35. Stanish, W.D., McCormack, R., Forriol, F., Mohtadi, N., Pelet, S., Desnoyers, J., Restrepo, A., and Shive, M.S. Novel scaffold-based BST-CarGel treatment results in superior cartilage repair compared with microfracture in a randomized controlled trial. J Bone Joint Surg Am **95,** 1640, 2013.
36. Hamanishi, M., Nakasa, T., Kamei, N., Kazusa, H., Kamei, G., and Ochi, M. Treatment of cartilage defects by subchondral drilling combined with covering with atelocollagen membrane induces osteogenesis in a rat model. J Orthop Sci **18,** 627, 2013.
37. van Susante, J.L., Buma, P., Schuman, L., Homminga, G.N., van den Berg, W.B., and Veth, R.P. Resurfacing potential of heterologous chondrocytes suspended in fibrin glue in large full-thickness defects of femoral articular cartilage: an experimental study in the goat. Biomaterials **20,** 1167, 1999.
38. Shao, X.X., Hutmacher, D.W., Ho, S.T., Goh, J.C., and Lee, E.H. Evaluation of a hybrid scaffold/cell construct in repair of high-load-bearing osteochondral defects in rabbits. Biomaterials **27,** 1071, 2006.
39. Breinan, H.A., Minas, T., Hsu, H.P., Nehrer, S., Sledge, C.B., and Spector, M. Effect of cultured autologous chondrocytes on repair of chondral defects in a canine model. J Bone Joint Surg Am **79,** 1439, 1997.
40. Agung, M., Ochi, M., Yanada, S., Adachi, N., Izuta, Y., Yamasaki, T., and Toda, K. Mobilization of bone marrow-derived mesenchymal stem cells into the injured tissues after intraarticular injection and their contribution to tissue

regeneration. Knee Surg Sports Traumatol Arthrosc **14,** 1307, 2006.
41. Wei, X., Gao, J., and Messner, K. Maturation-dependent repair of untreated osteochondral defects in the rabbit knee joint. J Biomed Mater Res **34,** 63, 1997.
42. Ahern, B.J., Parvizi, J., Boston, R., and Schaer, T.P. Preclinical animal models in single site cartilage defect testing: a systematic review. Osteoarthritis Cartilage **17,** 705, 2009.
43. Dai, L., He, Z., Zhang, X., Hu, X., Yuan, L., Qiang, M., Zhu, J., Shao, Z., Zhou, C., and Ao, Y. One-step repair for cartilage defects in a rabbit model: a technique combining the perforated decalcified cortical-cancellous bone matrix scaffold with microfracture. Am J Sports Med **42,** 583, 2014.
44. Hoemann, C.D., Sun, J., McKee, M.D., Chevrier, A., Rossomacha, E., Rivard, G.E., Hurtig, M., and Buschmann, M.D. Chitosan-glycerol phosphate/blood implants elicit hyaline cartilage repair integrated with porous subchondral bone in microdrilled rabbit defects. Osteoarthritis Cartilage **15,** 78, 2007.
45. Chen, H., Chevrier, A., Hoemann, C.D., Sun, J., Ouyang, W., and Buschmann, M.D. Characterization of subchondral bone repair for marrow-stimulated chondral defects and its relationship to articular cartilage resurfacing. Am J Sports Med **39,** 1731, 2011.
46. Poole, R., Blake, S., Buschmann, M., Goldring, S., Laverty, S., Lockwood, S., Matyas, J., McDougall, J., Pritzker, K., Rudolphi, K., van den Berg, W., and Yaksh, T. Recommendations for the use of preclinical models in the study and treatment of osteoarthritis. Osteoarthritis Cartilage **18 Suppl 3,** S10, 2010.
47. Case, N.D., Duty, A.O., Ratcliffe, A., Muller, R., and Guldberg, R.E. Bone formation on tissue-engineered cartilage constructs in vivo: effects of chondrocyte viability and mechanical loading. Tissue Eng **9,** 587, 2003.

Address correspondence to:
Tomohiro Onodera, MD, PhD
Department of Orthopaedic Surgery
Hokkaido University Graduate School of Medicine
Kita-15 Nishi-7
Sapporo
Hokkaido 060-8638
Japan

E-mail: tomozou@med.hokudai.ac.jp

Received: March 16, 2015
Accepted: August 27, 2015
Online Publication Date: November 3, 2015